

## APPENDIX A: Real Gas Models for Gamma

PAB3D has an improved model to handle the conservation of total enthalpy. The PAB3D code used the single ideal perfect gas (Air) assumption. In our modification, we changed the code to have a Variable Gamma. However, there may be a severe consequence in using this modification in preserving total enthalpy for internal flow calculation. We were not able to simulate flow at high temperature (1100 R) without using very small CFL (Courant-Fredrick-Lewy) number. Several cases do not converge with even small CFL. We have addressed the most important issue in preserving total enthalpy, which improves the convergence rate with a higher CFL number. We solved the enthalpy-energy equation as a function of temperature. However, the pressure and enthalpy used in the governing equations are not compatible with the real gas formulations. For ideal and real gas simulations enthalpy is related to internal energy through the following relation:

$$e = \text{internal energy} = h(T) - RT \dots\dots\dots(1)$$

where, h is the local enthalpy, R is the equivalent gas constant and T is the gas exact temperature.

Additionally, we also know that

$$R = \sum_{m=1}^{nspec} R_m \dots\dots\dots(2)$$

$$h(T) = \sum_{m=1}^{mspec} h_m = e + RT$$

$$e = \frac{E - 0.5\rho(u^2 + v^2 + w^2)}{\rho} \dots\dots\dots(3)$$

$$e(T) = h(T) - RT$$

where, nspec is the number of species that we are simulating. We have used McBride<sup>§</sup> formulation for perfect gases to evaluate total enthalpy as:

$$h_m = h_m^f + R_m \{b_1 + a_2 \ln T + \sum_{n=1, n \neq 2} \frac{a_n}{n-2} T^{n-2}\}_m \dots\dots\dots(4)$$

Where,  $h_m^f$  is heat of formation of 298.15 K, J/mol,  $R_m$  is the Gas Constant for each species,  $a_2$  and  $a_n$  are polynomial constants,  $b_1$  is the integration constant of the C polynomial:

$$\{C_p\}_m = \left\{ \sum_{n=1}^7 a_n T^{n-2} \right\}_m \dots\dots\dots(5)$$

$$C_v(T) = \sum_{m=1}^{nspec} \{C_p\}_m - R$$

<sup>§</sup> Bonnie J. McBride and Sanford Gordon, "Computer Program for Calculation of Complex Chemical Equilibrium Compositions and Applications", NASA LeRC TP-1311, June 1996.

For most of the elements, McBride obtained the coefficients in the above equations by means of a least-squares fit. The gas table has three intervals that are 200 to 1000k, 1000 to 6000 K and 6000 to 20000 K for all the above coefficients. From the PAB3D solution at specific time step, we can evaluate the value of T that satisfies the above 4 equations. Using Newton-Raphson iteration technique, we can find the root for the e(T) equation as

$$T(k) = T(k - 1) - (e(T) - e) / C_v(T) \dots\dots\dots(5a)$$

or,

$$T(k) = T(k - 1) - (h(T) - e - RT) / C_p(T) \dots\dots\dots(5b)$$

where, k is the iteration number. We stop the iterations when (e(T)-e)/C<sub>v</sub> is less than 1K, evaluate C<sub>v</sub> from the above equation and γ

$$\gamma = \frac{C_v + R}{C_v} \dots\dots\dots(6)$$

We have originally proposed the following approach to evaluate enthalpy and pressure in the governing equations

1. Use the correct form of the heat conductive term in the energy equation:

$$H_d = \frac{\mu}{P_r} \left( \frac{\partial h}{\partial x_i} \right), \quad h = H(T)$$

In the original code, the enthalpy (h) takes the following form:

$$h = C_p T = \frac{\gamma RT}{\gamma - 1} \text{ and } R = \sum_{i=1}^{nspec} C_i R_i$$

$$\{C_p\}_m = \left\{ \sum_{n=1} a_n T^{n-3} \right\}_m \dots\dots\dots(7)$$

$$C_v(T) = \sum_{m=1}^{nspec} \{C_p\}_m - R$$

2. Use the correct form in evaluating the pressure as:

$$P = \rho RT$$

In the original code, the pressure takes the following form:

$$P = \rho (\gamma - 1) e \dots\dots\dots(8)$$

This is based on the assumptions that e=C<sub>v</sub>T. We can then combine equations 2 & 3 to get e+RT = e+P/ρ = h, which is valid for Real and Ideal Gases

Let's now introduce a new variable Γ not to be confused with the specific heat ratio γ.

$$h = \Gamma e \dots\dots\dots(9)$$

Thus,

$$P = \rho(\Gamma - 1)e = \rho RT \dots\dots\dots(10)$$

and

$$h = \frac{\Gamma R}{(\Gamma - 1)} T \dots\dots\dots(11)$$

From equation 2 and the value of e, we can evaluate  $\Gamma = h/e$  and return it to the main code. We have used equations 10 and 11 to evaluate both P and h. This approach will not require any change of Ideal Gas CFD code as  $\Gamma$  replaces  $\gamma$  through out the entire code.

The user can specify either using the fixed or the variable temperature model through IMODEL in the Spec Cont segment of the user Control file. If

- IMODEL = 0, use the fixed temperature to evaluate  $\gamma$  (old model)
- IMODEL = 1, use the variable temperature model in evaluating  $\gamma$  by solving the enthalpy and heat coefficient equations (5a).
- IMODEL = 2, use the variable temperature model in evaluating  $\gamma$  by the solving the enthalpy and heat coefficient equations (5b).
- IMODEL = 3, use the variable temperature model in evaluating  $\Gamma$  by solving the enthalpy heat coefficient equations and evaluate  $\Gamma$  (5b and 9).

### A.1 Real Gas Supersonic Duct

This is a variable area duct of a ratio of 1.9. The grid geometry was given to AS&M Inc. by GEAE to evaluate the new Real gas model and compared with the theoretical values. We have fixed inflow pressure and velocity as well as the area ratio  $A2/A1$ . We have simulated two conditions at 685 and 840 K respectively. We have solved the Euler equations to avoid any viscous effect in the final solution. However the duct was not designed to avoid generating shocks inside the duct. **Table A-1** shows the conditions selected for the present simulations.

In general, all the models produce the same results qualitative. The real gas (1) generates much higher temperature as compared with the other models. **Table A-2** shows the comparisons between the predictions of the three models and the theoretical values. The real gas (3) predicted exit temperature, T2, and Mach # very close to the theoretical values for both flow conditions. The error was less than 0.5% that may be the contribution of the

Table A-1. Supersonic Duct Flow Conditions

	Condition 1	Condition 2
P1, N/m2	101235	101235
A2/A1	1.9	1.9
T1, K	685	840
U1, m/sec	600	600

Table A-2. Real Gas Predictions

	<b>Ideal gas Theory</b>	<b>Ideal gas Pab3d</b>	<b>Real Gas Theory</b>	<b>Real Gas (1) PAB3D</b>	<b>Real Gas (3) PAB3D</b>
T2, K (685)	448	450	458	494	460
M2 (685)	2.15	2.14	2.11	2.04	2.10
T2, K (840)	533	535	556	609	558
M2 (840)	2.14	2.13	2.074	2.002	2.08

shock wave generated inside the duct. The real gas (1) case was at least 10% of the theoretical values in both cases.

## APPENDIX B: MPI Implementation

### B.1 Cluster Machine Performance (more results will be forthcoming)

Tables B-1, B-2, and B-3 show samples of the cluster machine performance using MPI implementation of PAB3D for a balanced 3Block 3D Case with scalar diagonalization, Roe scheme, and single direction viscosities..

Table B-1. MPI PAB3D with Two-Equation Turbulence Model: 1,018,368 cells

Machine	CPU	MFLOPS	Total time/cell/itr (micro sec)	Percent speed up	Total time/cell/itr (× Single C-90)
Cray C-90 (f90)	1	360	12.0	NA	1
DEC Alpha 21164 533 MHz (Linux)	3	225	19.5	298	1.6
SGI Origin 2000 R10k 195 MHz	3	180	23.5	325	2.0
SGI R10k 195 MHz Octane	3	133	32.6	275	2.7
DEC Alpha 21164 533 MHz (Linux)	1	75	58.1	NA	4.8
SGI Origin 2000 R10k 195 MHz	1	56	76.4	NA	6.4
SGI R10k 195 MHz Octane	1	48	89.8	NA	7.5
Sun Ultra-2 200 MHz	1	43	99.2	NA	8.3

Table B-2. MPI PAB3D Two-Equation Turbulence Model: 127,296 cells (Table B-1 case, but with 1/8th the cells)

Machine	CPU	MFLOPS	Total time/cell/itr (micro sec)	Percent speed up	Total time/cell/itr (× Single C-90)
Cray C-90 (f90)	1	320	12	NA	1
DEC Alpha 533 MHz (Linux)	3	229	17	282	1.4
SGI Origin 2000 R10k 195 MHz	3	213	17.5	291	1.5
SGI R10k 195 MHz Octane	3	167	23	278	1.9
DEC Alpha 533 MHz (Linux)	1	80	48	NA	4.0
SGI Origin 2000 R10k 195 MHz	1	74	51	NA	4.3
SGI R10k 195 MHz Octane	1	60	64	NA	5.3
Sun Ultra-2 200 MHz	1	41	93	NA	7.8

Table B-3. MPI PAB3D with Laminar Model. 127,296 cells (Table B-2 case, but without Turbulence)

Machine	CPU	MFLOPS	Total time/cell/itr (micro sec)	Percent speed up	Total time/cell/itr (× Single C-90)
Cray C-90 (f90)	1	350	8	NA	1
DEC Alpha 533 MHz (Linux)	3	241	11.6	293	1.45
SGI Origin 2000 R10k 195 MHz	3	227	12.3	292	1.54
SGI R10k 195 MHz Octane	3	175	16	287	2
DEC Alpha 533 MHz (Linux)	1	81	34	NA	4.3
SGI Origin 2000 R10k 195 MHz	1	78	36	NA	4.5
SGI R10k 195 MHz Octane	1	60	46	NA	5.8
Sun Ultra-2 200 MHz	1	48	58	NA	7.2

### B.2 Introduction and Approach for Distributed Computers (MPI) in the PAB3D Code

The MPI prototype of the PAB3D code has the following characteristics.

- A communication interface (Buffer)

- Global-iteration gathering
- Message passing interface using either LAM/MPI 6.1 or MPICH
- Single source code for distributed or single computer compatibility

In order to understand the MPI implementation and the use of a communication interface (Buffer) in the PAB3D code, we need to discuss its communication data base structure. Each block contains six faces as:

$J_{\min}$ , =====	Face 1	$J_{\max}$ , =====	Face 2
$K_{\min}$ , =====	Face 3	$K_{\max}$ , =====	Face 4
$I_{\min}$ , =====	Face 5	$I_{\max}$ , =====	Face 6

One or more sub-faces may present each of these faces. This defines the local ID of each sub-face as Block 1, Face 3 and sub-face 4. Each of these sub-faces is assigned a global ID (Patch #). This is only done for Block communication sub-faces. **Fig. B-1** shows the example of transforming from local to global and back to local.

The database allows the communications across cells, faces and blocks with a universal set of information. The information is written as an unstructured list of cell correspondences over the block interface. Each entry contains four items; the address of

A-Cell (Destination, NB1) and B-Cells (Sources, NB2), the value of the contact area as a fraction of the total cell face area of A-Cell (Frc), and the total area of A-Cell. This information is collected at the fine grid level. This database provides cell area information sufficient for any level of grid density reduction. The NB1, NB2 and Frc have a fixed number of items (NITM) for the corresponding patch.

Similar to the database structure, we created for each patch a buffer with a size equal to:

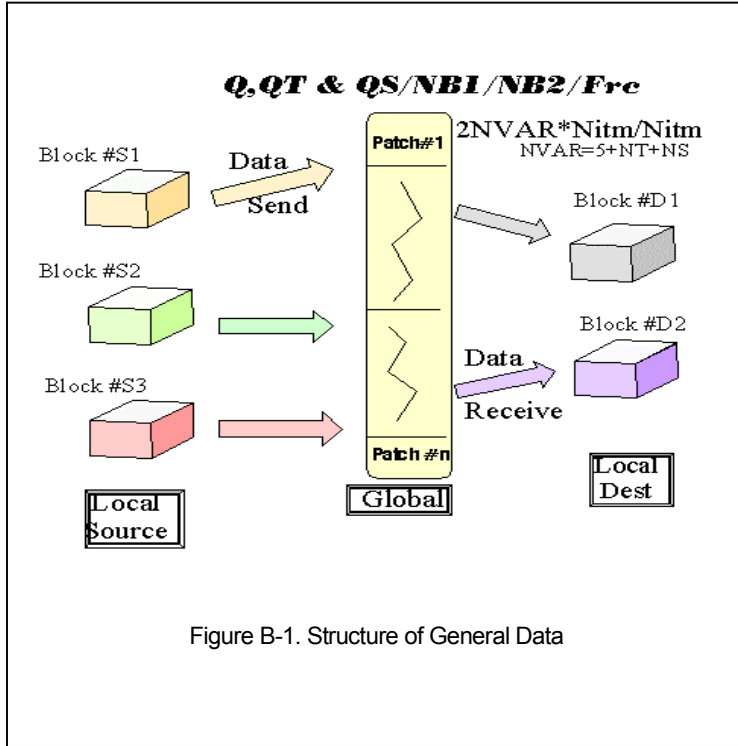
$2 * NVAR * NITM$ , where,  
 $NVAR = 5 + NT + NS$

NT, number of turbulent equations

NS, number of multi-species

Each of the source blocks is assigned a number of patches with their global Ids. Each of these blocks sends the Q, QT and QS to the corresponding patch location in the buffer. The blocking send is used to fill the buffer. We have used the MP\_BARRIER till all the needed variables are sent to the buffer. Then, the destination block collects all the variables from the global locations and put them in the related local location (face and sub-face). A non-blocking receive (IRECIEVE) is used to collect the data. This is very fast receiving MPI operation. However, we found that DEC Alpha computers have problems using the IRECIEVE. The entire operation is done without the need of the source block to know what is the receiving block or vice versa. Basically, there is no need for synchronize send and receive operations (very expensive send or receive MPI operations).

**Fig. B-1**, shows the BC, Gathering and Broadcasting in the PAB3D MPI prototype. The N processors (computers) are numbered from P0 to PN-1. The main job of the P0 processor is the I/O and data manipulations. The P0, then, broadcasts all the necessary information to the rest of the processors. This is a one-time operation at the beginning of a new solution. At the end of each global iteration (# local iterations), the P0 processor gathers the data from the other processors. Each processor solves one or more than one block. After one or more block



iteration, the boundary conditions are sent to the buffer. Later, each block will collect the boundary conditions from the buffer using the global ID.

**B.3 Test Cases using PAB3D MPI**

The R10000 195 MHz SGI computers at the Configuration Aerodynamic Branch are used in the present simulations. Each of these computers has a speed close to 1/6<sup>th</sup> of the Cray C90 computer. We have selected two test cases for the evaluation of the PAB3D MPI. First case represents a two-dimensional real gas simulation. The second case is three-dimension flow simulation. The second problem is a million grids 3D flow. Each case uses the standard two-equation turbulence model to simulate the viscous effect. These cases are not designed for efficient load balance using MPI.

**Case 1: Five (5) Blocks 2D Nozzle with Real Gas Simulation (50,000 Grid Points)**

A 50,000 grids and two-dimensional flow simulation of 3 gases flow is the first test case. We have used single and up to 3 processors in the evaluation of the PAB3D prototype. Using more than three processors will not add any speed because there are two blocks with sizes more than 33%.

Single processor performance: 57µs/grid point

MPI Performance

BCT 3%

GT 0.65%

Speed Increase 250%

Efficiency 83%

Multi processor performance 22.75 µs/grid point

BCT is the Boundary Conditions Time as ratio of total time.

GT is the Gathering Time as ratio to total time

Speed increase is the ratio between a single processor to the multiprocessors time

Efficiency is the (single processor time/(# processor \* multiprocessor time)

Table B-4. Case 1 Grid distribution

Block #	%
1	3.7
2	35.9
3	38.4
4	20.1
5	1.9

Table B-5. Case 1 Load Distribution

P	Blocks	Load %
0	2	35.9
1	3	38.4
2	1 4 5	25.7

**Case 2: Nine (9) Blocks 3D Nozzle Simulation (1,000,000 Grid Points)**

A 1,000,000 grids and three-dimensional flow simulation of Nozzle/Jet Plume flow is the second test case. We have used single and up to 4 processors in the evaluation of the PAB3D prototype.

Single processor performance: 90 ms/grid point

MPI Performance for 3 Processors

BCT 2.5%

GT 0.45%

Speed Increase 252%

Efficiency 84%

Multi processor performance 35.7  $\mu$ s/grid point 50% of C90 Speed

MPI Performance for 4 Processors

BCT 2.3%

GT 0.46%

Speed Increase 330%

Efficiency 82%

Multi processor performance 27.7  $\mu$ s/grid point 69% of C90 Speed

Table B-6. Case 2 Grid distribution

Block #	%
1	8.4
2	9.6
3	18.5
4	27.4
5	27.4
6	1.7
7	1.8
8	2.6
9	2.6

Table B-7. Case2 Load Distribution using 3 Processors

P	Blocks	Load %
0	1 2 3	36.5
1	5 6 8	31.7
2	4 7 9	31.8

Table B-8. Case2 Load Distribution using 4 Processors

P	Blocks	Load %
0	1 2 6 9	22.4
1	3 7 8	23.0
2	4	27.3
3	5	27.3



## APPENDIX C: Example Problem

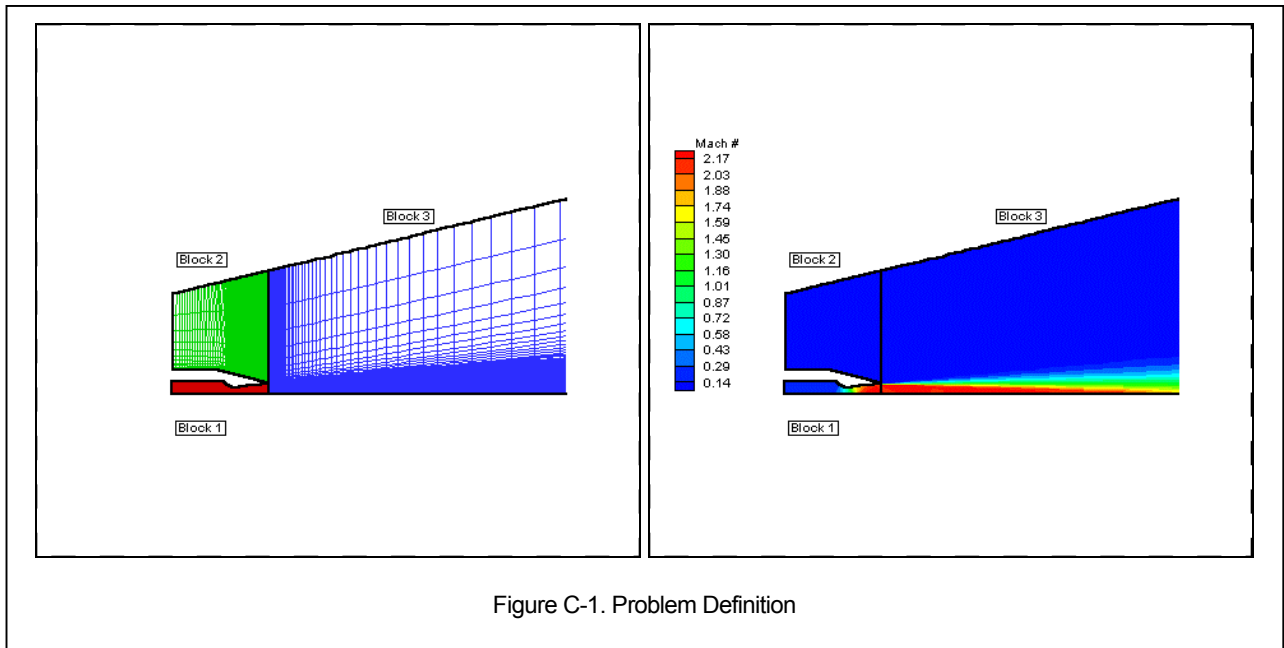


Figure C-1. Problem Definition

This case involves a "submerged" Supersonic jet emanating from an axisymmetric convergent-divergent Mach 2.2 nozzle. This nozzle was studied by J.M. Eggers in 1962. Velocity profiles and eddy viscosity distributions were obtained within the jet. The working fluid is air and the nozzle is operated at the pressure ratio corresponding to perfect expansion.

This case uses the grid and experimental data included in the NPARC code validation archive and the Wind validation archive.

### C.1 Solver Control File

```

#!PAB3D 100
  "Grid File"
axinoz01.g
  "Restart File"
restart.d
  "INIT File"
'init.d' 'user.cont'
  nte   year   Flg Hr:Mnt
    0       98 '0 00:00'
    nzone   ichk  ischeme
      1       3     4
    ngit   isafe  iauto
      2       0     0

nit
100 100
nitz
  1  1
#Blocks Block# idim jdim kdim nitb nseq  dt  dtmb
      3
1    189    59    2    1    111  -1.0  0.0

```

```

2      189      25      2      1      111      -1.0      0.0
3      149      107      2      1      111      -1.0      0.0
####Block 1: (188,58,1)
  ivfxj  ivflux irst  ivisc  kturb  ibs  ibf
  1      3      2      10      6      1      188
i-order  i-lmt j-order  j-lmt k-order  k-lmt  ibias
  3      2      3      2      3      2      0
  ncut-Imin  ncut-Imax  Imin & Imax Faces
  1      1
  ibci  j1  j2  k1  k2
  -11  1  58  1  1
10035  1  58  1  1
  ncut-Jmin  ncut-Jmax  Jmin & Jmax Faces
  1      1
  ibcjk  k1  k2  i1  i2
  -17  1  1  1  188
  0  1  1  1  188
  ncut-Kmin  ncut-Kmax  Kmin & Kmax Faces
  1      1
  ibcjk  j1  j2  i1  i2
  -17  1  58  1  188
  -17  1  58  1  188
####Block 2: (188,24,1)
  ivfxj  ivflux irst  ivisc  kturb  ibs  ibf
  1      3      2      10      6      1      188
i-order  i-lmt j-order  j-lmt k-order  k-lmt  ibias
  3      2      3      2      3      2      0
  ncut-Imin  ncut-Imax  Imin & Imax Faces
  1      1
  ibci  j1  j2  k1  k2
  -1  1  24  1  1
10035  1  24  1  1
  ncut-Jmin  ncut-Jmax  Jmin & Jmax Faces
  1      1
  ibcjk  k1  k2  i1  i2
  0  1  1  1  188
  -1  1  1  1  188
  ncut-Kmin  ncut-Kmax  Kmin & Kmax Faces
  1      1
  ibcjk  j1  j2  i1  i2
  -17  1  24  1  188
  -17  1  24  1  188
####Block 3: (148,106,1)
  ivfxj  ivflux irst  ivisc  kturb  ibs  ibf
  1      3      2      10      6      1      148
i-order  i-lmt j-order  j-lmt k-order  k-lmt  ibias
  3      1      3      1      3      1      0
  ncut-Imin  ncut-Imax  Imin & Imax Faces
  3      1
  ibci  j1  j2  k1  k2
10016  1  58  1  1
  -17  59  82  1  1
10026  83  106  1  1
  -6  1  106  1  1
  ncut-Jmin  ncut-Jmax  Jmin & Jmax Faces
  1      1
  ibcjk  k1  k2  i1  i2
  
```

```

-17      1      1      1      148
-1      1      1      1      148
ncut-Kmin      ncut-Kmax      Kmin & Kmax Faces
      1      1
ibcjk      j1      j2      i1      i2
-17      1      106      1      148
-17      1      106      1      148
Axisymmetric Supersonic Nozzle
rj dt iflagts      fmax isym
0.0254 -1.00 -4      5.00 2
igrd iriso inorm kg1 kg2 iperfl jkswp impvis
11      8      1      1      5      0      0      1
      ibc i2d itrp
      0      0      1
ivrt istat sigl sigu gam itre
3      0      0.0 2.5 1.4 0
nprfile
0
    
```

**C.2 User's Control File**

```

'Begin Memo'
'End Memo'
'Begin Spec Cont'
1.0      ,3      , 'CO2'      'N2'      'Air'      0
      0.1 0.9 0.
      0.1 0.9 0.
      0.0 0.0 1.
'End Spec Cont'
'Begin Ginit Cont'
      iunit nblock      Ireg
      0      3      0
      ncut      jmin      jmax      kmin      kmax      iset
      1
      1      1      59      1      2      3
      1      1      25      1      2      2
      1      1      107      1      2      2
      nset      iinit
      3      1
      P0      T0      Mach      int      mut/mu      alpha      beta      gamma      iin
162.000 525.000 0.300 0.000 0.000 0.000 0.000 1.400 0
      P0      T0      Mach      int      mut/mu      alpha      beta      gamma      iin
14.700 525.000 0.010 0.000 0.000 0.000 0.000 1.400 0
      P0      T0      Mach      int      mut/mu      alpha      beta      gamma      iin
14.700 525.000 0.300 0.000 0.000 0.000 0.000 1.400 0
'End Ginit Cont'
'Begin KE Cont'
      ibk ilhg iord      dtf itk icomp      comp      Int      ut/ul      inl      icu      idmp
      1 -14 0      1.0 2 5      0      0.001 0.100 0 0 0
      2 -14 0      1.0 2 5      0      0.001 0.100 0 0 0
      3 3 0      1.0 2 5      0      0.001 0.100 0 0 0
'End KE Cont'
'Begin Surf Cont'
ib,ifc1,ict, bcf1,bcf2,bcf3,bcf4,bcf5
    
```

```

2 1 1 0.145 0.15 90. 1. 0.4
'End'End Surf Cont'
'Beg'Begin Tran Cont'
Number of Blocks with Trip Points & Trip K- Int
      2 5.0000001E-02
Block Number & Number of I-Planes
      1 1
Number of Points for Plane #1
      1
Location J K I (for the finest grid)
      8 0 1
Block Number & Number of I-Planes
      5 1
Number of Points for Plane #1
      1
Location J K I (for the finest grid)
      8 0 1
'End'End Tran Cont'
'Beg'Begin Bc Cont'
  iunit  nblock  Ireg
      0      3      0
  ncut   jmin   jmax   kmin   kmax   iset
      1
      1      1   59      1      2      1
      1      1   25      1      2      2
      1      1  107      1      2      2
  nset   iinit
      3      1
  P0     T0     Mach   int  mut/mu  alpha  beta  gamma  iin
162.000 525.000 0.300 0.000 0.000 0.000 0.000 1.400 0
  P0     T0     Mach   int  mut/mu  alpha  beta  gamma  iin
14.700 525.000 0.010 0.000 0.000 0.000 0.000 1.400 0
  P0     T0     Mach   int  mut/mu  alpha  beta  gamma  iin
14.700 525.000 0.300 0.000 0.000 0.000 0.000 1.400 0
'End'End Bc Cont'
'Beg'Begin Perf Cont'
'End'End Perf Cont'
'Beg'Begin MPI Cont'
prc# #nbl bll-blbn
0 2 2 4
1 3 1 3 5
'End'End MPI Cont'

```

## APPENDIX D: Bibliography

1. Abdol-Hamid, K. S.: Development of Three-Dimensional Code for the Analysis of Jet Mixing Problem. NASA CR 4200, December 1988.
2. Abdol-Hamid, K.S.: Three-Dimensional Calculations for Underexpanded and Over expanded Supersonic Jet Flows, AIAA Paper 89-2196, September 1989.
3. Abdol-Hamid, K. S.: The Application of 3D Marching Scheme for the Prediction of Supersonic Free Jets. AIAA/ASME/SAE/ASEE 25th Joint Propulsion Conference, Monterey, CA July 1989.
4. Abdol-Hamid, K. S. and Compton, W. B, III: Supersonic Navier-Stokes Simulations of Turbulent Afterbody Flows. AIAA 7th Applied Aerodynamics Conference, AIAA 89-2194, Seattle, Washington August 1989.
5. Abdol-Hamid, K.S.: A Multiblock/Multizone code (PAB3D-v2) for the Three-Dimensional Navier-Stokes Equations: Preliminary Applications, NASA CR-182032, 1990.
6. Lakshmann, B. and Tiwari, S. N.: Application of an Improved Two-Equation Turbulence Model for Compressible Mixing Layer/Jet Plumes. Progress Report under Research Contract NAS1-18584-106 Old Dominion University November 1990.
7. Pao, S. P.; and Abdol-Hamid, Khaled S.: Application of a New Adaptive Grid for Aerodynamic Analysis of Shock Containing Single Jets. AIAA Paper 90-2025, AIAA/SAE/ASME/ASEE 26th Joint Propulsion Conference, Orlando, FL, July 1990.
8. Compton, W.B.,III and Abdol-Hamid, K.S.: Navier-Stokes Simulations of Transonic Afterbody Flows with Jet Exhaust, AIAA Paper 90-3057, August 1990.
9. Abdol-Hamid, K.S.: Application of a Multiblock/Multizone Code (PAB3D) for The Three-Dimensional Navier-Stokes Equations. 27th Joint Propulsion Conference AIAA 91-2155, Sacramento, California June 1991.
10. Uenishi, K. and Abdol-Hamid, K.: A Three-Dimensional Upwinding Navier-Stokes Code with k- $\epsilon$  Model for Supersonic Flows", AIAA 22nd Fluid and Plasmadynamic Conference, AIAA 91-1669, June 1991.
11. Compton, W. B, III and Abdol-Hamid, K. S.: Navier-Stokes Simulation of Nozzle -Afterbody Flows With Jets at Off Design Conditions. AIAA 91-3207, September 1991.
12. Pao, S. P.; and Abdol-Hamid, K. S.: Grid Adaptation to Multiple Functions for Applied Aerodynamic Analysis, Proceedings of the Third International Conference on Numerical Grid Generation, Barcelona, Spain, June 1991.
13. Abdol-Hamid, Khaled S.; Carlson, John R.; Pao, S. Paul: Computational Analysis of Vented Supersonic Exhaust Nozzles Using a Multiblock/Multizone Strategy. AIAA Paper No. 91-0125. 29th Aerospace Sciences Meeting, January 7-10, 1991.
14. Carlson, John R.; and Abdol-Hamid, Khaled S.: Prediction of Internal Performance for Two-Dimensional Convergent-Divergent Nozzles. AIAA Paper No. 91-2369, AIAA/SAE/ASME/ASEE 27th Joint Propulsion Conference, June 24-27, 1991.
15. Pao, S. Paul; Abdol-Hamid, Khaled S.; and Carlson, John R.: Computational Investigation of Circular-To-Rectangular Transition Ducts. AIAA Paper No. 91-3342, AIAA 9th Applied Aerodynamics Conference September 23-25, 1991.
16. Jones, W. T. and Walkley, K. B.: Numerical Investigation for Drag Reduction on a Single Engine Body-Engine Model, DEI Report D-396, 1992.
17. Abdol-Hamid, Khaled S.; Uenishi, K.; Carlson, John R.; Keith, B. D.: Commercial Turbofan Engine Exhaust Nozzle Flow Analysis Using PAB3D. AIAA Paper 92-2701. AIAA 10th Applied Aerodynamics Conference, June 22-24, 1992.
18. Compton, W. B., III; Abdol-Hamid, K. S. and Abeyounis, W. K.: Comparison of Algebraic Turbulence Models for Flows with Jet Exhaust. AIAA Journal, Vol. 30 No. 11, November 1992.
19. Carlson, John R.: A Nozzle Internal Performance Prediction Method. NASA TP-3221, 1992. Format(s): [Postscript](#), or [PDF](#)
20. Lakshmann, B. and Abdol-Hamid, K. S.: Application of Space Marching Procedure for Transport Equation of Turbulence Models. Computational Fluid Dynamics Journal, Vo. 1. No.3, October 1992.

21. Lakshmann, B. and Abdol-Hamid, K. S.: Comparative Study of Two Codes With an Improved Two-Equation Turbulence Model for Predicting Jet Plumes. 10th Applied Aerodynamics Conference, Palo Alto, California June 1992.
22. Jones, W. T. and Abdol-Hamid K. S.: Computational Analysis of Drag Reduction Techniques for Afterbody/Nozzle/Empennage Configurations. Aerospace Technology Conference and Exposition, Long Beach, California September 1992.
23. Abdol-Hamid, K. S.; Uenishi, K.; Keith, B. D.; and Carlson, John R.: Commercial Turbofan Engine Exhaust Nozzle Flow Analyses. Journal of Propulsion and Power, Vol. 9, No. 3, May-June 1993.
24. Carlson, John R.; and Abdol-Hamid, Khaled S.: Prediction of Static Performance for Single Expansion Ramp Nozzles. AIAA Paper No. 93-2571, AIAA/SAE/ASME/ASEE 29th Joint Propulsion Conference, June 28-30, 1993.
25. Carlson, John R.; Abdol-Hamid, K. S.; and Pao, S. Paul: Computational Analysis of Vented Supersonic Exhaust Nozzle Using a Multiblock/Multizone Strategy. Journal of Propulsion and Power, (tentative) Vol. 9, No. 6, November-December 1993.
26. Carlson, John R.: Analytic Prediction of Isolated Performance of an Axisymmetric Nozzle at  $M = 0.90$ . NASA TM-4506, 1993.Format(s): [Postscript](#), or [PDF](#)
27. Pao, S. P.; Carlson, J. R.; and Abdol-Hamid, K. S.: Computational Investigation of Circular-to-Rectangular Transition Ducts. Journal of Propulsion and Power, Volume 10, Number 1, January-February 1994, pp. 95-100.
28. Carlson, J. R.; Computational Prediction of Isolated Performance of an Axisymmetric Nozzle at Mach Number 0.90. NASA TM-4506, February 1994.
29. Kuhne, C. M.; Uenishi, K.; Leon, R. M.; Abdol-Hamid, K. S.; CFD Based 3D Aero Analysis System for High-Speed Mixer-Ejector Exhaust Nozzles. AIAA 94-2941, 30<sup>th</sup> AIAA/ASME/SAE/ASEE Joint Propulsion Conference, Indianapolis, IN, June 27-29, 1994.
30. Giuliano, V. J.; Flugstad, T. H.; Semmes, R.; and Wing, D. J.: Static Investigation and Computational Fluid Dynamics (CFD) Analysis of Flowpath Cross-Section and Trailing-Edge Shape Variations in Two Multi-axis Thrust Vectoring Nozzle Concepts. AIAA 94-3367, 30<sup>th</sup> AIAA/ASME/SAE/ASEE Joint Propulsion Conference, Indianapolis, IN, June 27-29, 1994.
31. Carlson, J. R.; and Asbury, S. C.: Two-Dimensional Converging-Diverging Rippled Nozzles at Transonic Speeds. NASA TP-3440, July 1994.
32. Lakshmanan, B.; and Abdol-Hamid, K. S.: Investigation of Supersonic Jet Plumes Using an Improved Two-Equation Turbulence Model. Journal of Propulsion and Power, Volume 10, Number 5, September-October 1994, pp. 736-741.
33. Alexander, Kristina L. : Investigation of a Supersonic Cruise Nozzle. 45th Annual Southern Region Student Conference, 1994. as a NASA Technical Paper
34. Lakshmanan, B.; and Abdol-Hamid, K. S.: Investigation of Supersonic Jet Plumes Using an improved Two-Equation Turbulence Model. Journal of Propulsion and Power, Vol. 10, No. 5, September 1994.
35. Lakshmanan, B.; Chylek, T.; and Tiwari, S. N.: Application of Nonlinear  $k-\epsilon$  Model to Supersonic Separated Flows. AIAA 95-0228, 33rd Aerospace Sciences Meeting and Exhibit, Reno, NV, January 9-12, 1995.
36. Abdol-Hamid, K. S.; Lakshmanan, B.; and Carlson, J. R.: Application of Navier-Stokes Code PAB3D with  $k-\epsilon$  Turbulence Model to Attached and Separated Flows. NASA TP-3480, January 1995. Format(s): [Postscript](#), or [PDF](#)
37. Abdol-Hamid, K. S.; Carlson, J. R.; and Pao, S. P.: Calculation of Turbulent Flows Using Mesh Sequencing and Conservative Patch Algorithm. AIAA 95-2336, 31st AIAA/ASME/SAE/ASEE Joint Propulsion Conference and Exhibit, San Diego, CA, July 10-12, 1995
38. J. F. Federspiel, L. S. Bangert, D. J. Wing and T. Hawkes, Fluidic Control of Nozzle Flow---Some Performance Measurements , 31st AIAA/ASME/SAE/ASEE Joint Propulsion Conference, San Diego, California, AIAA Paper No. 95-2605, July 10-12, 1995, Format(s): [Postscript](#), or [PDF](#).
39. Carlson, J. R.; Pao, S. P.; Abdol-Hamid, K. S.; and Jones, W. T.: Aerodynamic Performance Predictions of Single and Twin Jet Afterbodies. AIAA 95-2622, 31st AIAA/ASME/SAE/ASEE Joint Propulsion Conference and Exhibit, San Diego, CA, July 10-12, 1995. Format(s): [Postscript](#), or [PDF](#)
40. "Aerodynamics of 3-D Aircraft Afterbodies ", AGARD Advisory Report No. 318, September 1995.

41. Abdol-Hamid, K. S.: Implementation of Algebraic Stress Models in a General 3-D Navier-Stokes Method (PAB3D). NASA CR-4702, December 1995.
42. Deere, K. A.: An Experimental and Computational Investigation of a Translating Throat Single Expansion-Ramp Nozzle. Thesis for Master of Science for the George Washington University. December 1995.
43. William B. Compton III, Comparison of Turbulence Models for Nozzle-Afterbody Flows With Propulsive Jets , NASA TP-3592, September 1996, pp. 117, Format(s): [Postscript](#), or [PDF](#)
44. Capone, F. J.; Asbury S. C.; and Deere, K. A.: Experimental and Computational Induced Aerodynamics from Missile Jet Reaction Controls at Angles of Attack to 75 Degrees. AIAA 96-2479, 14th AIAA Applied Aerodynamics Conference, New Orleans, LA, June 18-20, 1996.
45. Carlson, J. R.; Reubush D. E.: High Reynolds Number Analysis of an Axisymmetric Afterbody with Flow Separation. AIAA 96-2274, 19th AIAA Advanced Measurement and Ground Testing Technology Conference, New Orleans, LA, June 17-20, 1996.
46. Deere, K. A.; and Asbury, S. C.: An Experimental and Computational Investigation of a Translating Throat Single Expansion-Ramp Nozzle. AIAA 96-2540, 32<sup>nd</sup> AIAA/ASME/SAE/ASEE Joint Propulsion Conference & Exhibit, Lake Buena Vista, FL, July 1-3, 1996. Format(s): [Postscript](#), or [PDF](#)
47. Midea, A. C.; Austin, T.; Pao, S. P.; DeBonis, J. R.; and Mani, M.: High Speed Civil Transport (HSCT) Isolated Nacelle Transonic Boattail Drag Study and Results Using Computational Fluid Dynamics (CFD). HSR025, February 1996.
48. Carlson, J. R.: High Reynolds Number Analysis of Flat Plate and Separated Afterbody Flow Using Non-Linear Turbulence Models. AIAA 96-2544, 32<sup>nd</sup> AIAA/ASME/SAE/ASEE Joint Propulsion Conference and Exhibit, Lake Buena Vista, Florida, Jult 1-3, 1996. Format(s): [Postscript](#), or [PDF](#)
49. Pao, S. Paul and Abdol-Hamid, K. S.: Numerical Simulation of Jet Aerodynamics Using Three-dimensional Navier-Stokes Method (PAB3D). NASA TP-3596, September 1996. Format(s): [Postscript](#), or [PDF](#)
50. Lakshmann, B.; Tiwari, S. and Abdol-Hamid, K.: Prediction of High Speed Free-Shear Flows Using High-Order Turbulence Models. AIAA 97-0762, 35<sup>th</sup> Aerospace Conference and Exhibit, Reno, NV, January 6-9, 1997.
51. Hunter, C.: Experimental, Theoretical, and Computational Investigation of Separated Nozzle lows. AIAA 98-3107, 34<sup>th</sup> AIAA/ASME/SAE/ASEE Joint Propulsion Conference & Exhibit, Cleveland, OH, July 13-15, 1998.
52. Karen A. Deere, PAB3D Simulations of a Nozzle With Fluidic Injection for Yaw Thrust-Vector Control , 34th AIAA/ASME/SAE/ASEE Joint Propulsion Conference and Exhibit, Cleveland, Ohio, AIAA 98-3254, July 13-15, 1998, pp. 12 Format(s): [Postscript](#), or [PDF](#)
53. John R. Carlson, Prediction of Very High Reynolds Number Compressible Skin Friction , 20th AIAA Advanced Measurement and Ground Testing Technology Conference, Albuquerque, New Mexico, AIAA 98-2880, June 15-18, 1998, (2MB). Format(s): [Postscript](#), or [PDF](#)
54. Qunzhen Wang, Steven J. Massey, Khaled S. Abdol-Hamid and Neal T. Frink, Solving Navier-Stokes Equations With Advanced Turbulence Models on Three-Dimensional Unstructured Grids , 37th AIAA Aerospace Sciences Meeting and Exhibit, Reno, Nevada, AIAA 99-0156, January 11-14, 1999, Format(s): [Postscript](#), or [PDF](#)
55. Deere, K. and Asburty, S.: Experimental and Computational Investigation of a Translating-Throat, Single-Expansion-Ramp Nozzle. NASA TP-1999-209138, May 1999. [PDF File](#)
56. Hunter, Craig A. and Deere, Karen A. "Computational Investigation of Fluidic Counterflow Thrust Vectoring". AIAA 99-2669, presented at the 35th Annual AIAA/ASME/SAE/ASEE Joint Propulsion Conference, Los Angeles, CA, June 20-23, 1999.
57. Hunter, C. and Deere, K.:Experimental Investigation of Convolved Contouring for Aircraft Afterbody Drag Reduction. 35th AIAA/ASME/SAE/ASEE Joint Propulsion Conference and Exhibit. AIAA 99-2670, June 1999 [PDF](#)
58. Duquesne N.; Carlson,J.R.; Rumsey,C.L. and Gatski,T.B.: Computation of Turbulent Wake Flows in Variable Pressure Gradient, 30th AIAA Fluid Dynamics Conference, June 28 - July 1, 1999, Norfolk, VA, AIAA 99-3781
59. Deere, K. :Computational Investigation of the Aerodynamic Effects on Fluidic Thrust Vectoring. 36th AIAA/ASME/SAE/ASEE Joint Propulsion Conference and Exhibit. AIAA 2000-3598, July 2000. Format(s): [Postscript](#) or [PDF](#)

60. Carlson, J.R.; Duquesne, N.; Rumsey, C.L.; Gatski, T.B.: Computation of turbulent wake flows in variable pressure gradient. *Computers & Fluids* 30 (2001) 161-187.
61. Kenrick, W.: An Experimental and Computational Investigation of Multiple Injection Ports in a Convergent-Divergent Nozzle for Fluidic Thrust Vectoring. Master degree Thesis, George Washington University, 2001
62. Thomas, R. H.; Kinzie, K. W.; and Pao, S. P. :Computational Analysis of a Paylon-Cheveron Core Nozzle Interaction. AIAA 2001-2185, May 2001.
63. Massey, S.; and Kenrick, W.: Computational Analyses of Propulsion Aeroacoustics for Mixed Flow Nozzle Pylon Installation at Takeoff. To be published as NASA CR, 2001.
64. Capone, F. J and Deere, K. :Transonic Investigation of Two-Dimensional Nozzles Designed for Supersonic Cruise. AIAA 2001-3199, 37th AIAA/ASME/SAE/ASEE Joint Propulsion Conference and Exhibit, July 2001.



